SISO Control Strategy of Resonant Dual Active Bridge with a Tuned CLC Network

Meiqi Wang[1], Bo Yang[2], Lie Xu[3], Jing Li[1], David Gerada[4], Chunyang Gu[1], He Zhang[1], Chris Gerada[1,4], Yongdong Li[3]
[1]THE UNIVERSITY OF NOTTINGHAM NINGBO CHINA
[2]XI'AN UNIVERSITY OF TECHNOLOGY
[3]TSINGHUA UNIVERSITY
[4]THE UNIVESITY OF NOTTINGHAM
Ningbo, China
Xi'an, China
Beijing, China
Nottingham, United Kingdom
E-Mail: Meiqi.Wang@nottingham.edu.cn

Acknowledgements

This work was supported by the Zhejiang Natural Science Foundation under Grant LY19E070002 and LQ19E070002 and by the Zhejiang Provincial Department of Human Resources and Social Security under Grant QJD1803013.

Keywords

«Bidirectional DC/DC converter», «RDAB», «Control Design», «Modeling», «System Efficiency»

Abstract

This paper proposed a linear state-space model for a resonant dual active bridge with a tuned capacitor-inductor-capacitor network which is applied to an energy storage system. The proposed model is used for predicting the behavior of the proposed system and estimated the state variables under large signal variation. Using the proposed model, a decoupled control strategy was designed which realizes the high frequency link currents control and also improves the efficiency of the converter. By applying the steady-state relationship between state variables and the system inputs, the controller was simplified to a single proportional integral (PI) controller instead of from three PI controllers, which was implemented on a low cost digital signal processor and verified experimentally.

Introduction

Recently, dual active bridges (DABs) have received an increasing attention due to their bidirectional power transmission and galvanic isolation capabilities, which can provide a high power density and accommodate a wide range of voltages by operating in both buck and boost modes. Early DAB converters were controlled using single-phase-shift (SPS) control to allow for bidirectional power transfer at variable power levels, which can easily achieve soft switching when the magnitudes of the two ac voltages are matched by the transformer ratio. However, when the converter is operated outside of the proper voltage range, the zero-voltage switching (ZVS) can hardly be achieved and the peak current will increase which then lead to an increase of switching and conduction losses [1]. In order to reduce the switch current stresses and the attendant switching and conduction losses, many other complicated control strategies have been proposed [2] [3] which have shown an improved soft switching range and lower conduction losses, however, these methods usually require more complicated control systems and still have a large reactive current at rated power.

In order to improve the soft switching range, a number of quasi-resonant type DAB topologies, consisting of series resonant networks, have been investigated [4] [5]. The most common resonant dual active bridge (RDAB) topology is the series RDAB (SRDAB) [6] - [8], which has received an increasing attention due to it low requirement of resonant network components and its inherent dc blocking

capability. However, it needs a wide switching frequency range to modulate the power transfer, which make the design of controller and filter being more complicated.

Regardless of control and resonant schemes employed, the existing DABs typically requires a more complex control system, particularly when they operate with wide load and supply voltage variations. In this paper, based on linear state-space model and mathematical analysis, a simplified decoupled control strategy for a capacitor-inductance-capacitor (CLC) tuned resonant DAB is proposed and implemented with a single PI controller which achieves the control of both the primary and secondary ac current amplitudes while ensuring soft switching of the switches at a wide voltage range. An experimental prototype is designed and operated in various conditions to investigate the performance of the control scheme.

Basic operation of the RDAB

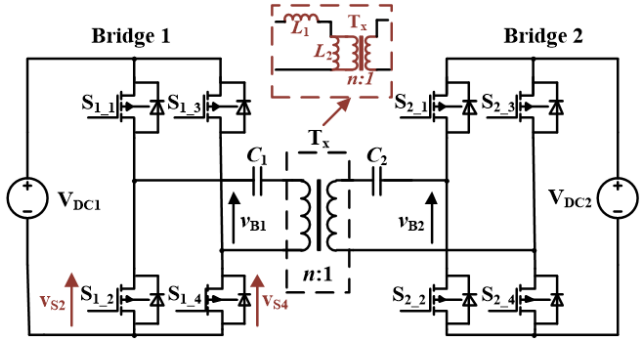

Fig. 1 Resonant dual active bridge

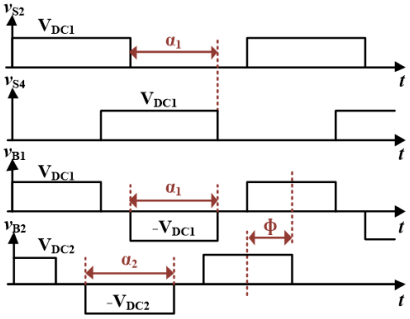

Fig. 2 TPS modulation strategy

The structure of capacitor-inductor-capacitor (CLC) RDAB is shown in Fig. 1. Two additional capacitors C_1 and C_2 is added to the primary side and secondary side of transformer T_x, respectively, which then act as an integral part of resonant network with T_x 's leakage and mutual inductance L_1 and L_2. The two full-bridge converters are controlled using a Three Phase Shift (TPS) modulation scheme as demonstrated in Fig.2. The switches of each leg are controlled to have a duty cycle of 50% and the output of the first leg is phase shifted from the output of the second leg by α_1 for the primary bridge and α_2 for the second bridge. The output of the secondary full-bridge v_2 is phase shifted from the output of the primary full-bridge v_1, to lead v_1 by ϕ. The outputs of the full-bridge converter have been simplified into voltage source v_{B1} and v_{B2}, which are represented by the Fourier series in (1) and (2).

$$v_{B1} = V_{DC1}\frac{4}{\pi}\sum_{b_1=1,3\ldots}^{n}\frac{1}{b_1}\cos(b_1\omega_s t)\sin\left(\frac{b_1\alpha_1}{2}\right) \tag{1}$$

$$v_{B2} = V_{DC2}\frac{4}{\pi}\sum_{b_2=1,3\ldots}^{n}\frac{1}{b_2}\cos(b_2\omega_s t + b_2\varphi)\sin\left(\frac{b_2\alpha_2}{2}\right) \tag{2}$$

The magnitude of the power transferred has been quantified in a previous paper by the author [9], which was shown that majority of the power was transferred at the fundamental frequency of the tuned resonant network. The tuned network presents a high impedance to harmonics generated by the converters. Consequently, the effects of these harmonics on the power transfer will be insignificant and therefore ignoring harmonics, the magnitude of the power can be simplified to (3):

$$P = \frac{8nV_{DC1}V_{DC2}}{\pi^2 L_2}\sin(\varphi)\sin\left(\frac{\alpha_2}{2}\right)\sin\left(\frac{\alpha_2}{2}\right) \tag{3}$$

Mathematical analysis of RDAB

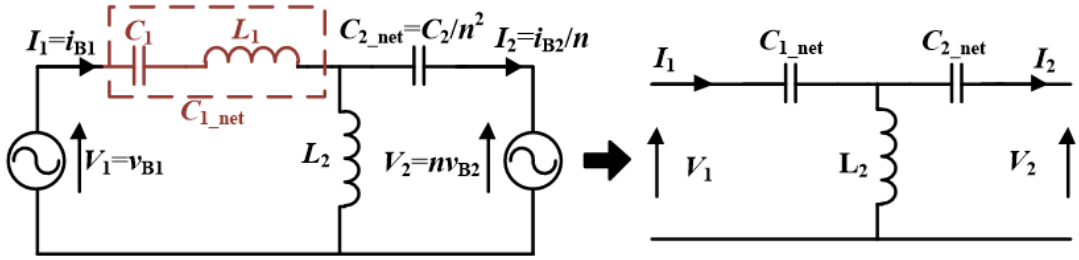

Fig. 3 Equivalent circuit model of RDAB (a) at fundamental frequency (b) at HF ac link

In order to simplify the mathematical analysis, the converter works at fundamental frequency is simplified as shown in Fig.3 (a), where the voltage across C_1 and L_1 behaves as a capacitor (C_{1_net}) voltage. Then the fundamental circuit at switching frequency is illustrated in Fig.3 (b) while circuit resistance have a relatively insignificant effect on the current and will, therefore, be ignored and their losses can be allowed for late, then the relationships between original circuit and the equivalent circuit are shown as follows:

$$Z_1 = -jX_{C1_{net}} = -j\left(X_{C_1} - X_{L_1}\right) \tag{4}$$

$$Z_2 = -jX_{C2_{net}} = -jn^2X_{C_2} \tag{5}$$

$$Z_3 = jX_{L_2} \tag{6}$$

The resonant network consisted with C_{1_net}, C_{2_net} and L_2 is tuned to the fundamental of the switching frequency f_s as follow:

$$X_{1_{net}} = X_{2_{net}} = \frac{1}{\omega_s C_{1_{net}}} = \frac{1}{\omega_s C_{2_{net}}} = \omega_s L_2 = X_{L_2} \tag{7}$$

Substituting (7) to (4) to (6), the following relationship among T-equivalent circuit (shown in Fig. 4(a)) was found:

$$Z_1 = Z_2 = -Z_3 = -j\omega_s L_2 = \frac{n^2}{j\omega_s C_2} \tag{8}$$

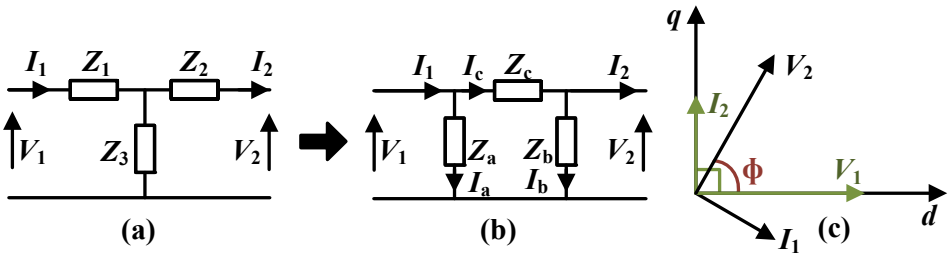

Fig. 4 Equivalent circuit and steady-state voltage and current phasors at fundamental frequency of resonant DAB (a) T-equivalent circuit (b) delta-equivalent circuit (c) voltage and current phasors

To recognize the relationship between bridge currents, i_1 and i_2, and voltages, v_1 and v_2, a delta-equivalent circuit of resonant network is illustrated in Fig. 4(b), where the independences are calculated as follows:

$$Z_a = Z_b = -Z_c = Z_1 + Z_3 + \frac{Z_1 Z_3}{Z_2} = j\omega_s L_2 \tag{9}$$

According to KVL and KCL of delta network and the inductances relationship (9), at the switching frequency and steady-state, the bridge current can be calculated as shown in (10) and (11), which shows that i_1 is decoupled with v_1 and i_2 is decoupled with v_2 (as shown in Fig. 4c).

$$I_1 = I_a + I_c = (\frac{1}{Z_a} + \frac{1}{Z_c})V_1 - \frac{1}{Z_c}V_2 = \frac{1}{j\omega_s L_2}V_2 \tag{10}$$

$$I_2 = I_c + I_b = -(\frac{1}{Z_b} + \frac{1}{Z_c})V_2 + \frac{1}{Z_c}V_1 = -\frac{1}{j\omega_s L_2}V_1 \tag{11}$$

To investigate the effects that the modulation variables have on the current, (1) and (2) have been substituted into (10) and (11), the magnitudes of the high frequency link current i_1 and i_2 are abstained as (12) and (13), where it can be found that the magnitudes of currents i_1 and i_2 are controlled by the phase shift α_2 and $\alpha_1$respectively.

$$|I_1| = \frac{4nV_{DC2}}{\pi\omega_s L_2}\sin\left(\frac{\alpha_2}{2}\right) \tag{12}$$

$$|I_2| = -\frac{4nV_{DC1}}{\pi\omega_s L_2}\sin\left(\frac{\alpha_1}{2}\right) \tag{13}$$

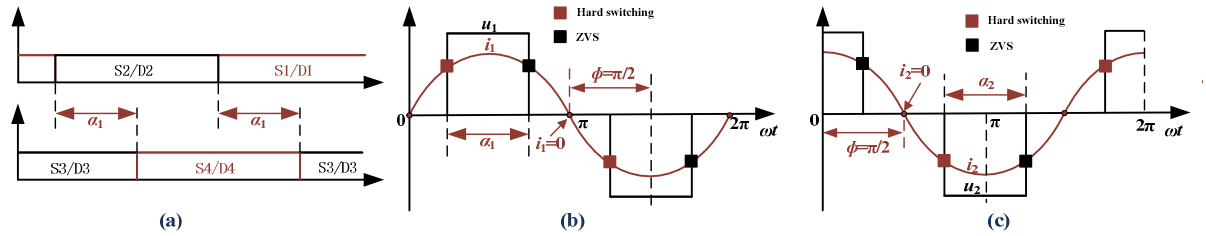

Fig.5 Relationship among pulse width, voltages and currents (a) primary switch states (b) primary voltage and currents waveforms (c) secondary voltage and currents waveforms

The relationships between the voltages and currents in (10) and (11) are illustrated in Fig. 4(c), where i_2 is fixed to lead v_1 by 90° and v_2 is fixed to lead i_1 by 90°. As it can be seen that when ϕ is fixed at 90° or -90° (depending on the power flow direction), the currents of the bridges (i_1 and i_2) will align to the voltages (v_1 and v_2), which then results in unity power factor (UPF) at the ac terminals of both full-bridge converters. The relationship among pulse width, voltage and current is illustrated in Fig. 5, where α_1 controls the pulse width of v_1 and therefore the magnitude of the fundamental component of v_1, α_2 controls the pulse width of v_2, while ϕ controls the phase difference between v_1 and v_2.

According to the relationships between currents and voltages shown in Fig. 4(c), the voltage midpoint corresponds to the current starting point, it can be expressed as ϕ also controls the phase difference between i_1 and v_1, as well as the phase different between i_2 and v_2, which is illustrated in Fig 5. In UPF applications, ϕ is fixed at 90° or -90°, the power transfer is modulated using α_1 and α_2, the freedom of the system is simplified to two degrees.

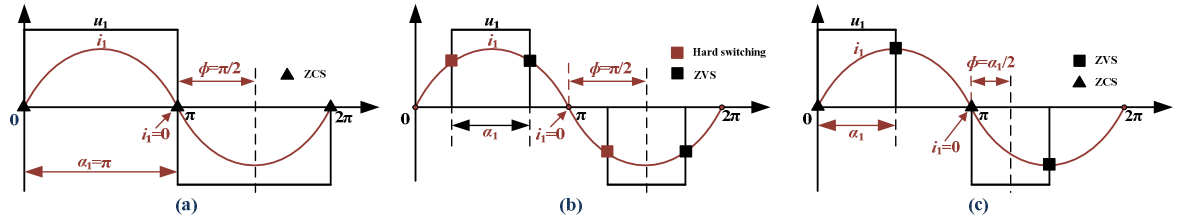

Fig. 6 Voltage and current under different modulations (a) at maximum power transfer capability (b) with modulation of α_1 and α_2, while φ fixed at $\pm\pi/2$ (c) with proposed modulation.

As shown in Fig. 6(a), in the maximum power transmission, the converter is zero-current switching or near ZCS, however, at the magnitude of power transfer is modulated down using α_1 and α_2, some of the switches start hard switching as can be seen in Fig. 6(b). This leads to an increase of the switching loss in high frequency link and a decrease of the power transmission efficiency of the system. From the analysis of Fig. 5, when the relationship among the three freedoms of the system can be implemented as (14), a wide power range of soft-switching can be achieved as shown in Fig. 6(c).

$$\varphi = \frac{\alpha_1}{2} = \frac{\alpha_2}{2} \tag{14}$$

Control scheme design of RDAB

The purpose of the RDAB control is to control the amplitudes of the currents in the resonant tank, i_1 and i_2, by α_1 and α_2, while ensuring soft switching of the switches by modulating ϕ. In order to simplify the control algorithm, the *d-q* decoupling control is introduced, and the *d*-axis is oriented in the direction of v_1, the relationship between the steady-state voltage and the phase angle in the *d-q* frame is derived as follows:

$$v_{1q} = 0 \tag{15}$$

$$v_{1d} = \frac{4}{\pi} V_{DC1} \sin\left(\frac{\alpha_1}{2}\right) = v_{1max} \sin\left(\frac{\alpha_1}{2}\right) \tag{16}$$

$$v_{2q} = \frac{4}{\pi} V_{DC2} \sin\left(\frac{\alpha_1}{2}\right) \sin\varphi = v_{2max} \sin\left(\frac{\alpha_1}{2}\right) \sin\varphi \tag{17}$$

$$v_{2d} = \begin{cases} \frac{4}{\pi} V_{DC2} \sin\left(\frac{\alpha_1}{2}\right) \cos\varphi & (\varphi \geq 0) \\ \frac{-4}{\pi} V_{DC2} \sin\left(\frac{\alpha_1}{2}\right) \cos\varphi & (\varphi < 0) \end{cases} = v_{2max} \sin\left(\frac{\alpha_1}{2}\right) \cos\varphi \tag{18}$$

Since v_{1q} is zero due to the selection of v_{1d} as the reference frame (as shown in Fig.4 (c)), v_{1d} is the only input that affects i_2 and the current i_2 lead v_1 by 90, the following assumptions can be made:

$$i_{2d} = 0 \tag{19}$$

$$i_{2q} = i_{2max} \sin(\frac{\alpha_1}{2}) \tag{20}$$

$$i_{1d} = i_{1max} \sin(\frac{\alpha_1}{2}) \sin\varphi \tag{21}$$

$$i_{1q} = i_{1max} \sin(\frac{\alpha_1}{2}) \cos\varphi \tag{22}$$

By submitting (14) to (15) - (22), the relationships between primary side and secondary side can be found as follows:

$$v_{2q} = \frac{v_{2max}}{v_{1max}^2} v_{1d}^2 \tag{23}$$

$$v_{2d} = \frac{v_{2max}}{v_{1max}} v_{1d} \sqrt{1 - \left(\frac{v_{1d}}{v_{1max}}\right)^2} \tag{24}$$

$$i_{1d} = \frac{i_{1max}}{i_{2max}^2} i_{2q}^2 \tag{25}$$

$$i_{1q} = \frac{i_{1max}}{i_{2max}} i_{2q} \sqrt{1 - \left(\frac{i_{2q}}{i_{2max}}\right)^2} \tag{26}$$

As it can be seen, v_{2q} and v_{2d} can be calculated by v_1, i_{1d} and i_{1q} can be calculated by i_{2q}, and the amplitude of i_{2q} or i_2 depends on v_1, the system transmission power can be adjusted by controlling the amplitude of α_1, whereby the degree of freedom of the system is reduced to 1. At the same time, the maximum soft switch control will be achieved. According to the above analysis, the input and output relationship of the AC system is directly related, the single-in-single-out (SISO) modulation algorithm is proposed, as shown in Fig. 7. α_1 and α_2 are varied to control the magnitudes of the currents i_1 and i_2, while ϕ will be varied along with the change to improve the soft switching range of the converter.

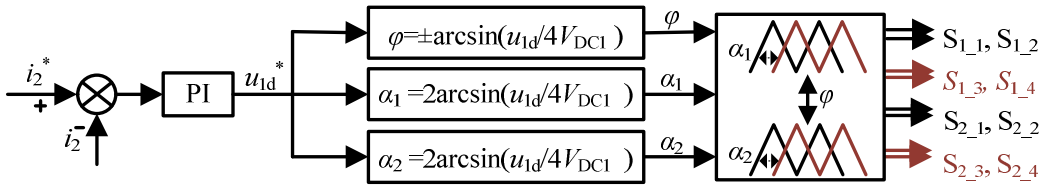

Fig. 7 SISO control scheme of CLC tuned RDAB

As mentioned before, the input of the AC system is directly related to the output, therefore, only the amplitude of i_{2q} which is the same as the amplitude of i_2 is needed for the control. This measurement can be easily realized through the use of an inexpensive current transformer (CT). Additionally, only one PI controller is implemented, the inputs for the other loops are derived from (23) - (26), which make the RDAB being more flexible for complicated applications like hybrid DC-AC microgrid which is enabled by energy storage systems.

Experimental results

An experimental prototype of CLC tuned RDAB was designed to investigate the performance of the control strategy and the mathematical analysis (as shown in Fig. 8). In Fig. 10, the voltage and current waveforms of the primary and secondary H bridges with varying phase shifts are illustrated. From Fig.10, all the switches in the primary and secondary full bridges realize the soft switching. The power throughput and efficiency of the prototype RDAB under various modulation levels are shown in Fig. 9. The maximum efficiency of the system is observed at rated power and is approximately 96%. Furthermore, the system efficiency is maintained well above 82% even at lower modulation factors, which suggest a significant improvement in performance in comparison to conventional DAB converters.

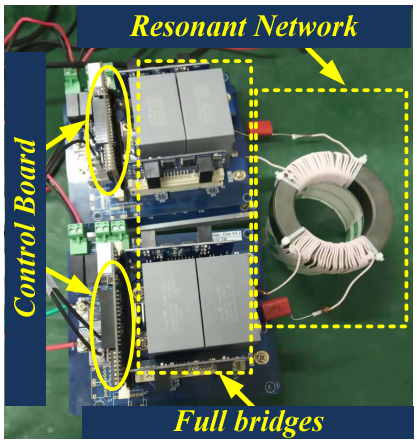

Fig. 8 Experimental prototype of CLC tuned RDAB

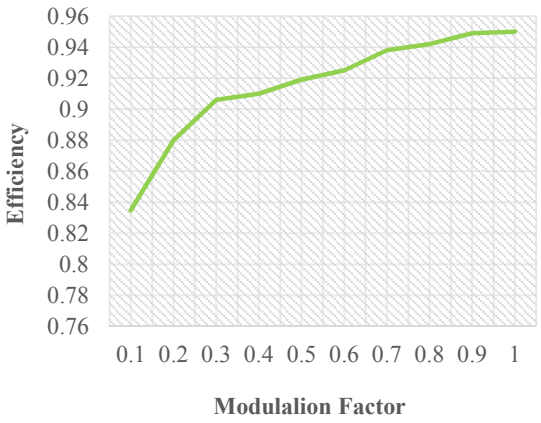

Fig. 9 Converter efficiency over the modulation range

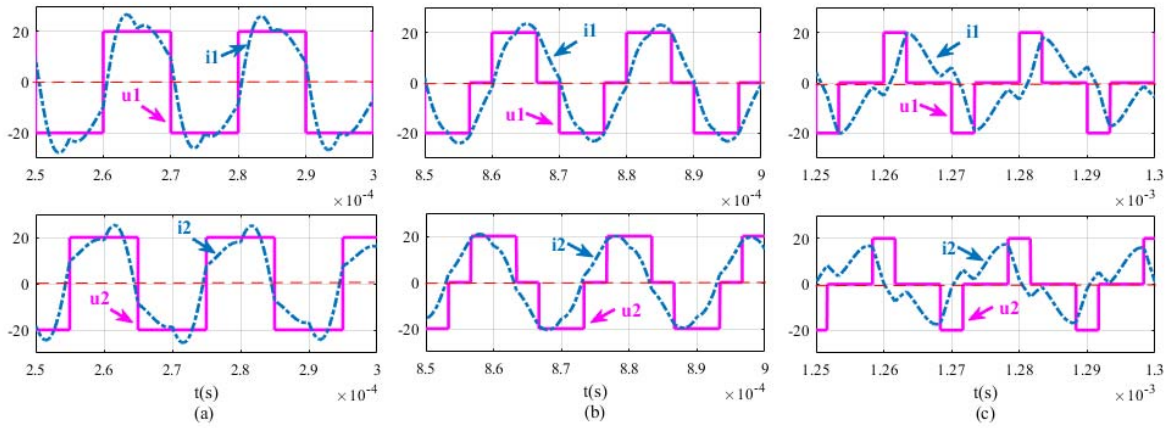

Fig. 10 Voltage and current waveforms under different modulation (a) $\alpha_1 = \alpha_2 = 2$ $\phi = 180°$ (M=1) (b) $\alpha_1 = \alpha_2 = 2$ $\phi = 120°$ (M=0.65) (c) $\alpha_1 = \alpha_2 = 2$ $\phi = 60°$ (M=0.125)

Conclusion

In this paper, a mathematical analysis has been presented to accurately predict the performance of the proposed SISO control strategy. Experimental results of a prototype RDAB, operated under various conditions, have been presented to demonstrate the improved performance of the converter. Results indicate that the proposed SISO control strategy for resonant DAB topology has a good closed-loop dynamic response and steady-state performance, while indicates a potential to further increase the operating efficiency by employing a purpose-designed transformer, which will be smaller than that of a conventional DBA converter on account of the lower operating currents.

References

[1] S. Inoue and H. Akagi.: A Bidirectional DC–DC Converter for an Energy Storage System with Galvanic Isolation, in IEEE Transactions on Power Electronics, vol. 22, no. 6, pp. 2299-2306, Nov. 2007.

[2] F. Krismer.: Accurate Small-Signal Model for the Digital Control of an Automotive Bidirectional Dual Active Bridge, in IEEE Transactions on Power Electronics, vol. 24, no. 12, pp. 2756-2768, Dec. 2009.

[3] W. Han.: Wide-Range ZVS Control Technique for Bidirectional Dual-Bridge Series-Resonant DC–DC Converters, in IEEE Transactions on Power Electronics, vol. 34, no. 10, pp. 10256-10269, Oct. 2019.

[4] R. P. Twiname.: A New Resonant Bidirectional DC–DC Converter Topology, in IEEE Transactions on Power Electronics, vol. 29, no. 9, pp. 4733-4740, Sept. 2014.

[5] M. Yaqoob.: Extension of Soft-Switching Region of Dual-Active-Bridge Converter by a Tunable Resonant Tank, in IEEE Transactions on Power Electronics, vol. 32, no. 12, pp. 9093-9104, Dec. 2017.

[6] J. Jung, H. Kim, M. Ryu and J. Baek, Design Methodology of Bidirectional CLLC Resonant Converter for High-Frequency Isolation of DC Distribution Systems, in IEEE Transactions on Power Electronics, vol. 28, no. 4, pp. 1741-1755, Apr. 2013.

[7] H. Kim, M. Ryu, J. Baek and J. Jung, High-Efficiency Isolated Bidirectional AC–DC Converter for a DC Distribution System, in IEEE Transactions on Power Electronics, vol. 28, no. 4, pp. 1642-1654, Apr. 2013.

[8] F. Ibanez, J. M. Echeverria and L. Fontan, Novel technique for bidirectional series-resonant DC/DC converter in discontinuous mode, in IET Power Electronics, vol. 6, no. 5, pp. 1019-1028, May 2013.

[9] R. Twainame, D. THrimawithana, U. Madawala, and C. Baguley, A dual active bridge topology with a tuned CLC network, IEEE Transaction on Power Electronics, vol.30, no. 12, pp. 6543-6540, Dec. 2015.